

A Comparative Study of Polypropylene Nucleated by Individual and Compounding Nucleating Agents. I. Melting and Isothermal Crystallization

Hongwei Bai,¹ Yong Wang,¹ Qin Zhang,² Li Liu,¹ Zuowan Zhou¹

¹Key Laboratory of Advanced Technologies of Materials (Ministry of Education), School of Materials Science and Engineering, Southwest Jiaotong University, Chengdu 610031, China

²State Key Laboratory of Polymer Materials Engineering, College of Polymer Science and Materials, Sichuan University, Chengdu 610065, China

Received 1 April 2008; accepted 14 August 2008

DOI 10.1002/app.29153

Published online 30 October 2008 in Wiley InterScience (www.interscience.wiley.com).

ABSTRACT: In this study, melting and isothermal crystallization behaviors of polypropylene (PP) nucleated with different nucleating agents (NAs) have been comparatively studied. α -phase NA 1,3 : 2,4-bis (3,4-dimethylbenzylidene) sorbitol (DMDBS, Millad 3988), β -phase NA aryl amides compound (TMB-5), and their compounds were introduced into PP matrix, respectively. The crystallization and melting characteristics as well as the crystallization structures and morphologies of nucleated PP were studied by differential scanning calorimetry (DSC), wide angle X-ray diffraction (WAXD), and polarized light microscopy (PLM). As indicated by previous work that a few amounts of α -phase NA (DMDBS) or β -phase NA (TMB-5) has apparent nucleation effect for PP crystallization. However, the crystallization of PP nucleated with compounding

NAs is dependent on the content of each NA. In the sample of PP with 0.1 wt % DMDBS and 0.1 wt % TMB-5, the nucleation efficiency of TMB-5 is much higher than that of DMDBS and PP crystallization is mainly nucleated by TMB-5, and in this condition, β -phase PP is the main crystallization structure. For the sample of PP with 0.2 wt % DMDBS and 0.2 wt % TMB-5, 0.2 wt % DMDBS has higher nucleation efficiency than 0.2 wt % TMB5, and α -phase is the main crystalline structure in this sample. The isothermal crystallization kinetics and crystallization structure have been analyzed in detail in this work. © 2008 Wiley Periodicals, Inc. *J Appl Polym Sci* 111: 1624–1637, 2009

Key words: polypropylene; nucleating agents; melting; isothermal crystallization; crystallization structure

INTRODUCTION

Polypropylene (PP), as one of the semicrystalline polymers, has been intensively researched in the last years because of its polymorphism characteristic (the monoclinic α -phase, the trigonal β -phase, the orthorhombic γ -phase, and finally the so-called smectic phase).^{1–7} Among all the crystalline forms of PP, the monoclinic α -phase and trigonal β -phase have attracted most interest because α -phase is the most common phase in melt-crystallized samples or articles and β -phase usually shows better impact toughness and drawability than α -phase.⁵ However, it is difficult to obtain high amount of β -phase in melt-crystallized samples. Shear field, temperature

gradients, and specific β -phase nucleating agent (NA) are proved to be in favor of the formation of β -phase.^{7–12}

Generally, the crystallization rate of semicrystalline polymers from the melted state depends on two factors: the nucleation rate and spherulites growth rate. NA as one of the additives presents a role of increasing the nucleation density of polymer greatly and enhancing the nucleation rate dramatically, so that it has been widely used in semicrystalline polymers processing to reduce the cycle time and sometimes improve the optical properties of such polymers.^{13–15} It has been shown that the presence of NA affects the polymer nucleation activation energy and the fold surface energy.^{16,17} A good NA reduces the interfacial surface free energy.¹⁸ In a certain condition, the presence of NA also affects the lamellar thickness and the spherulites growth rates of polymers.¹⁹

So far, at least two kinds of NAs, α -phase and β -phase NAs, have been developed for PP crystallization. α -phase NA improves the stiffness and optical properties of PP, and β -phase NA improves the PP toughness and heat distortion temperature. Much

Correspondence to: Y. Wang (yongwang1976@163.com).

Contract grant sponsor: National Natural Science Foundation of China (Youth Foundation); contract grant number: 50403019.

Contract grant sponsor: Sichuan Youthful Science and Technology Foundation (P. R. China); contract grant number: 07ZQ026-003.

work has been done to research the crystallization behavior and structure of PP with individual α -phase or β -phase NA.^{1-7,11-16} However, the melting, crystallization, and crystallization structure of PP with α/β compounding NAs are less researched.¹² In factually, it is very important to know which NA controls mainly PP crystallization when compounding NAs are introduced into PP, because the final crystallization structures, i.e., the ration of α -phase content to β -phase content, are determined by the nucleation efficiency of each NA.

In this work, sorbitol derivatives DMDBS and aryl amides compounds TMB-5 were introduced into PP simultaneously. Sorbitol derivatives are thought to be one group of the best efficient α -phase NAs for PP crystallization because they crystallize into nanofibrillar structures in the polymer melt and form a gel network structure through self-organization of these nanofibrillars.^{15,20-22} A high content of sorbitol and a low melt temperature are available for such gel network structure formation.^{21,23} Some work has been done to understand the effect of sorbitol gel network structure on crystallization and morphology of PP.^{14,24,25} In this work, the melting, isothermal crystallization behaviors, and crystallization structures of PP with individual NA and compounding NAs are comparatively investigated, respectively. It is expected that the results are not only in favor of the evaluating of nucleation efficiency of α -phase or β -phase NA, but also available for understanding how to control the crystallization structure of PP through adjusting the composition of compounding NAs.

EXPERIMENTAL

Materials

All the materials used in this study are commercially available. PP (F401, Langang Petrochemical, Lanzhou, China) with a melt flow rate (MFR) of 2.5 g/10 min (230°C/2.16 kg) was used as the matrix polymer. The α -phase NA 1,3 : 2,4-bis(3,4-dimethylbenzylidene) sorbitol (DMDBS, Millad 3988) was produced by Milliken Chemical, Belgium. The β -phase NA aryl amides compound (TMB-5) was supplied by Fine Chemicals Department of Shanxi Provincial Institute of Chemical Industry, China.

Sample preparation

To achieve the best dispersion of the NA in PP, a two-step process was employed to prepare the materials. Namely, a master batch of 5 wt % NA in PP was first prepared through melt blending of a NA and PP; and then, the master batch was melt blended with different contents of PP to obtain the

corresponding materials (PP with 0.1 wt % DMDBS, 0.2 wt % DMDBS, 0.1 wt % TMB-5, 0.2 wt % TMB-5, 0.1 wt % DMDBS and 0.1 wt % TMB-5, and 0.2 wt % DMDBS and 0.2 wt % TMB-5, shown as PP/0.1DM, PP/0.2DM, PP/0.1TM, PP/0.2TM, PP/0.1DM/0.1TM, and PP/0.2DM/0.2TM, respectively). The melt blending of such materials was carried out on a twin-screw extruder (TSSJ-25). During the extrusion, the screw speed was set as 120 r/min and the temperature was 150–200°C from hopper to die. Importantly, to ensure that the crystallization of PP is not affected by other additives except NA, no anti-oxidant was added into PP during processing. It could be believed that nearly no degradation of PP happened in our sample preparation because of the relative low processing temperature.

Differential scanning calorimetry

A PerkinElmer differential scanning calorimetry (DSC) Pyris-1 was used to study the isothermal crystallization and subsequent melting behaviors of sample. The instrument was calibrated with indium as a standard. For each measurement, about 8.0 mg sample was heated to 200°C quickly and maintained at this temperature for 5 min to eliminate the thermal history; then the sample was cooled down to a predetermined temperature at the cooling rate of 100°C/min, maintained at this temperature for enough time to leave the sample crystallization completely; and then the sample was cooled down to room temperature quickly; at last, the sample was heated again from room temperature to 200°C at the heating rate of 10°C/min.

Wide angle X-ray diffraction

Wide angle X-ray diffraction (WAXD, Panalytical X'pert PRO diffractometer with Ni-filtered CuK α radiation) was used to characterize the crystal structure of PP with compounding NAs. The sample was first heated to 200°C and maintained at this temperature for a long time to erase any thermal history, and then the sample was transferred to a hot stage with predetermined temperature to leave the sample crystallize completely. The continuous scanning angle range used in this study was from 5° to 35° at 40 kV and 40 mA. The β -phase fraction (K_β) in the sample was calculated from WAXD diffractograms according to the following relation²⁶:

$$K_\beta = I_{300}^\beta / (I_{110}^\alpha + I_{040}^\alpha + I_{130}^\alpha + I_{130}^\beta) \quad (1)$$

where I_{110}^α , I_{040}^α , and I_{130}^α are the integral intensities of the (110), (040), and (130) reflections of the α -phase, respectively, and I_{300}^β is the integral intensity of (300) reflections of β -phase.

Polarized light microscopy

Polarized light microscopy (XPN-203, China) with a hot-stage was used to characterize the crystallization morphologies of samples. First, a sample of about 5 mg was placed between two glass slides and was heated to melt completely, and then the sample was pressed to obtain a slice with the thickness of about 20 μm ; Second, the sample was transferred to the hot-stage with a predetermined temperature of 130°C and maintained at this temperature until the crystallization of sample was finished completely. The crystallization morphology of the sample was taken images via a digital camera.

RESULTS AND DISCUSSION

Melting behavior

Figure 1 shows the DSC heating curves of virgin PP and PP nucleated with different NAs (individual NA and compounding NAs) after isothermal crystallization at different temperatures as indicated. It can be observed that virgin PP sample presents double melting peak at about 149–155°C and 162–167°C, and the peak temperatures shift to high temperatures with the increase of crystallization temperature (T_c). The left melting peak is ascribed to the fusion of β -phase, and the right one to α -phase.^{13,27} The existence of a few amounts of β -phase PP in virgin PP sample after crystallized isothermally can be further demonstrated by WAXD result (shown by the arrow in Fig. 2). The formation of β -phase may be induced by catalyst residue in virgin PP. PP/0.1DM only presents single melting peak at about 164–168°C, indicating only α -phase formation with the presence of DMDBS. PP/0.2DM presents a main melting peak (α_1) at about 165°C and this melting peak keeps nearly invariant with increasing T_c . However, a weak melting peak (α_2) at about 167–170°C appears besides the main melting peak, and this shoulder peak becomes stronger with the increase of T_c , indicating more stable α -phase formation during the crystallization process or melting-recrystallization of α -phase with smaller size or poor perfection during the heating process.^{28–30} PP/0.1TM and PP/0.2TM present multiple melting peaks at \sim 155–159°C, 165–166°C, and 168–171°C (Shown as β , α_1 , and α_2 , respectively). Both the melting peaks of β and α_2 shift toward high temperatures with increasing T_c ; however, the melting peak of α_1 keeps nearly invariant. To the best of our knowledge, it is very difficult for PP crystallization to achieve 100% β -phase and the β -phase is unstable too. During the heating process, the unstable β -phase tends to melt first and recrystallize as α -phase with more stable crystal structure.^{28,31,32} From the heating curves of PP/0.1TM and PP/0.2TM, it can be deduced that the

melting peak α_1 is associated with the fusion of α -phase formed during the isothermal crystallization process, and melting peak α_2 is contributed to the fusion of reorganized α -phase from the melting of β -phase and poor perfect α -phase during the heating process. It is interesting to observe the melting behaviors of PP/0.1DM/0.1TM and PP/0.2DM/0.2TM samples. PP/0.1DM/0.1TM shows similar melting behaviors compared with PP/0.1TM, indicating the crystallization structure of the former sample formed during the crystallization process is similar to that of the latter one. Similarly, PP/0.2DM/0.2TM presents similar melting behaviors compared with PP/0.2DM, also indicating the similarity of crystallization structure formed during the isothermal crystallization process. But it should be noticed that α_2 peak of PP/0.2DM/0.2TM may be associated with the melting-recrystallization-melting of α -phase with smaller size or poor perfection and the fusion of reorganized α -phase from the melting of unstable β -phase during the heating process.

Making a comparison between β -phase melting peak temperatures of virgin PP and nucleated PP with the presence of TMB-5, the nucleated PP gives higher melting peak temperature than the virgin PP, which indicates that the β -phase formed in nucleated PP is more stable than that of virgin PP.

According to Hoffman–Weeks theory, the equilibrium melting temperature T_m^0 can be easily obtained from the following equation^{33,34}:

$$T_m = \Phi T_c + (1 - \Phi) T_m^0 \quad (2)$$

where T_m is the observed melting peak temperature, T_c is the isothermal crystallization temperature, and Φ is the stability parameter depending on the crystal thickness. The crystal structure is very stable for $\Phi = 0$ and inherently unstable for $\Phi = 1$. The smaller the Φ value, the more stable the crystal structure is. The T_m^0 values can be obtained by linear extrapolating the experimental data to $T_m = T_c$ line. Figure 3 shows the typical Hoffman–Weeks plots of virgin PP. The values of about 185.1 and 195.5°C correspond to the T_m^0 value of β -phase and α -phase, respectively. Similarly, the T_m^0 values of nucleated PP are obtained and the results are shown in Table I. Because the multiple melting peaks observed in the heating curves suggest the presence of different types of crystal structure, the T_m^0 values of such different structures are also deduced according to Hoffman–Weeks theory, and the results are also shown in Table I. It seems that the addition of NA reduces the T_m^0 value corresponding to the main melting peak of nucleated PP. (Marked by “*”) The Φ values of virgin PP and nucleated PP prove that α -phase is a stable crystallization structure and β -phase is an unstable one. It is necessary to point out that PP nucleated with individual NA or compounding NAs

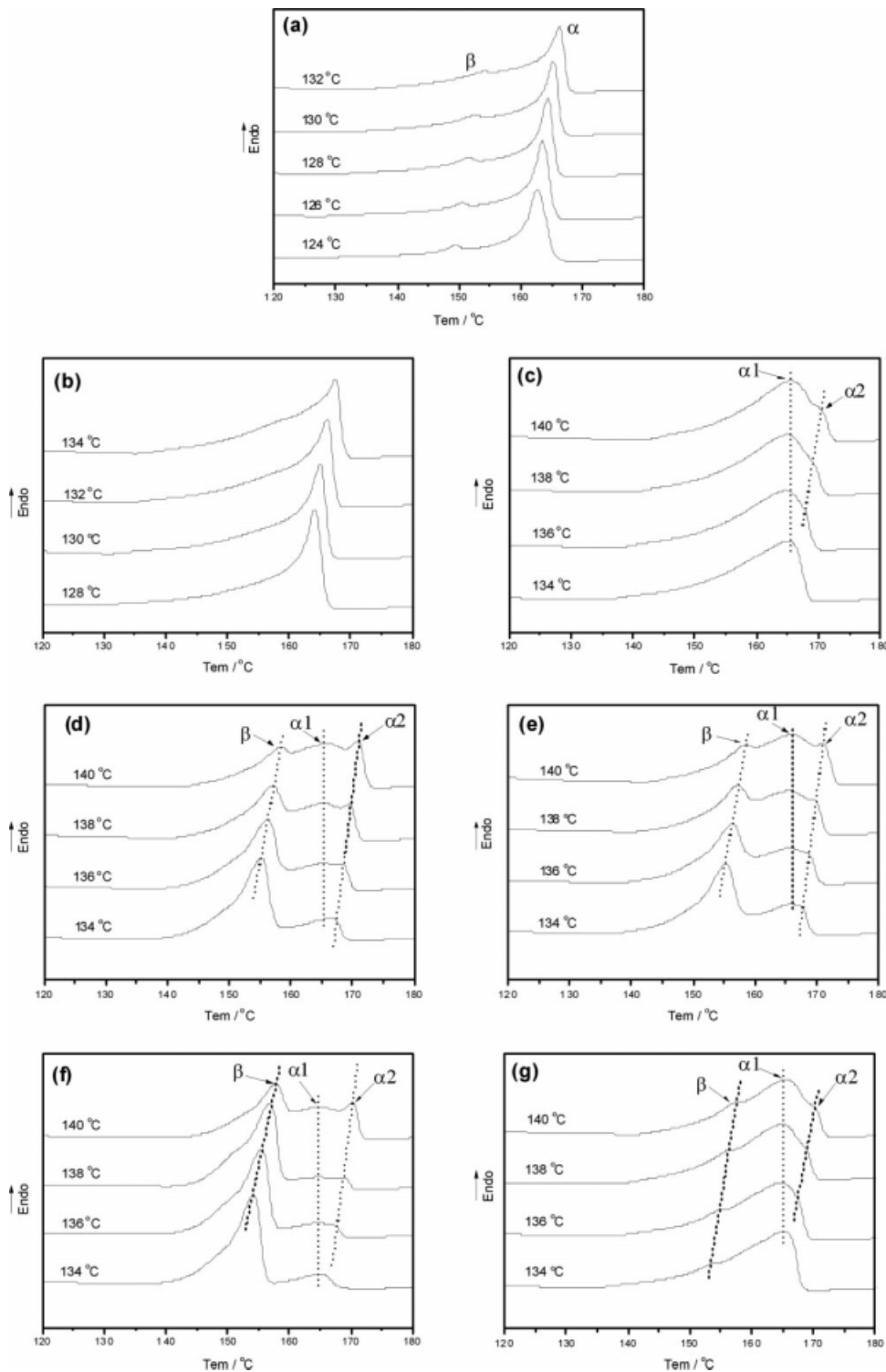


Figure 1 DSC heating curves of virgin PP and PP nucleated with different NAs, recorded at a heating rate of $10^{\circ}\text{C}/\text{min}$ after isothermal crystallization at the temperatures indicated. (a) Virgin PP, (b) PP/0.1DM, (c) PP/0.2DM, (d) PP/0.1TM, (e) PP/0.2TM, (f) PP/0.1DM/0.1TM, and (g) PP/0.2DM/0.2TM.

shows more stable crystallization structure compared with the corresponding crystallization structure in virgin PP. However, the addition of 0.1 wt % DMDBS reduces not only the crystallization structure stability in PP/0.1DM but also the β -phase stability in PP/

0.1DM/0.1TM. By the way, the Φ values deduced from the melting peak temperatures of α_2 do not represent the real structure stability because the melting peaks α_2 are related with the melting of β -phase and subsequent recrystallization process

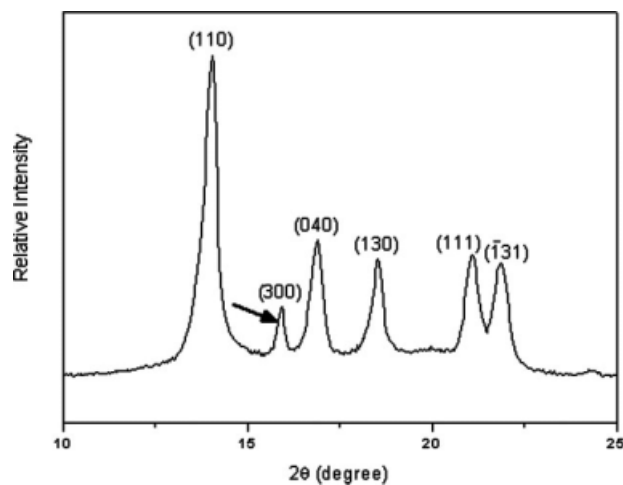


Figure 2 WAXD profile of virgin PP obtained through isotherm crystallization at 126°C.

(PP/0.1TM, PP/0.2TM, and PP/0.1DM/0.1TM) or the melting-recrystallization-melting process of unstable α -phase (PP/0.2DM and PP/0.2DM/0.2TM).

Isothermal crystallization kinetics

The isothermal crystallization behaviors of virgin PP and nucleated PP were investigated through DSC at different temperatures. The heat flow evolutions of such samples versus crystallization time are shown in Figure 4. Apparently, the crystallization of virgin PP is very slow [Fig. 4(a)]. Once NA is introduced into PP, the crystallization rate is enhanced greatly. In PP/0.1DM and PP/0.2DM, DMDBS content influences PP crystallization rate dramatically. High content of DMDBS results in much higher crystallization rate. But in PP/0.1TM and PP/0.2TM, the crystallization rate has no apparent change in the same crystallization temperature. Furthermore, one should notice from Figure 4 that PP/0.1TM shows higher crystallization rate than PP/0.1DM, but PP/0.2TM has lower crystallization rate than PP/0.2DM. Compounding NAs nucleated PP shows higher crystallization rate too. It is interesting to observe that

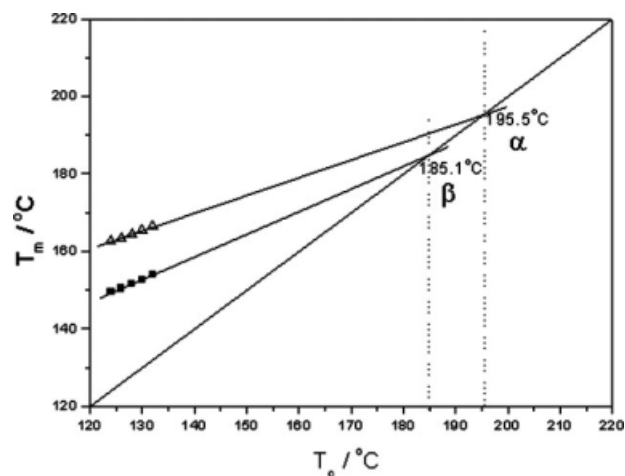


Figure 3 Plots of T_m (highest temperature of melting peak) versus T_c (isothermal crystallization temperature) for virgin PP.

the crystallization rate of PP/0.1DM/0.1TM is close to that of PP/0.1TM and much higher than that of PP/0.1DM, and the crystallization rate of PP/0.2DM/0.2TM is close to that of PP/0.2DM and much higher than that of PP/0.2TM.

Making a comparison of heat flow curves of PP/0.1DM and PP/0.2DM, one should notice another interesting crystallization phenomenon. The crystallization of PP/0.1DM is very slow in the early stage and abruptly becomes very fast in the later stage, and the heat flow curves show second exothermic peak at higher crystallization temperature. [Shown by arrows in Fig. 4(b)] However, PP/0.2DM shows faster crystallization in the early stage and becomes slower in the later stage. By the way, the exothermic peaks are very asymmetric whether for PP/0.1DM or for PP/0.2DM. [Shown as inserted graph in Fig. 4(b)].

The comparison of the relative crystallization fraction (X_c %) evolution curves at different crystallization temperatures are shown in Figure 5. Because of the relative lower crystallization rates of PP and PP/0.1DM compared with PP/0.1TM and PP/0.1DM/0.1TM, Figure 5(a,b) shows only X_c % of PP/0.1TM

TABLE I
Variation of Equilibrium Melting Temperature (T_m^0) of Virgin PP and PP Nucleated with Different NAs

Sample	$\alpha 1$		$\alpha 2$		β	
	T_m^0 (°C)	Φ	T_m^0 (°C)	Φ	T_m^0 (°C)	Φ
PP	195.5 ^a	0.460	–	–	185.1	0.585
PP/0.1DM	209.5 ^a	0.558	–	–	–	–
PP/0.2DM	172.2 ^a	0.210	215.1	0.600	–	–
PP/0.1TM	169.7	0.132	215.0	0.590	178.7 ^a	0.526
PP/0.2TM	169.9	0.129	214.9	0.588	181.1 ^a	0.549
PP/0.1DM/0.1TM	163.3	–0.051	258.1	0.744	186.9 ^a	0.620
PP/0.2DM/0.2TM	172.3 ^a	0.209	214.3	0.600	186.9	0.616

^a Data were used to calculate the lamellae thickness of the samples.

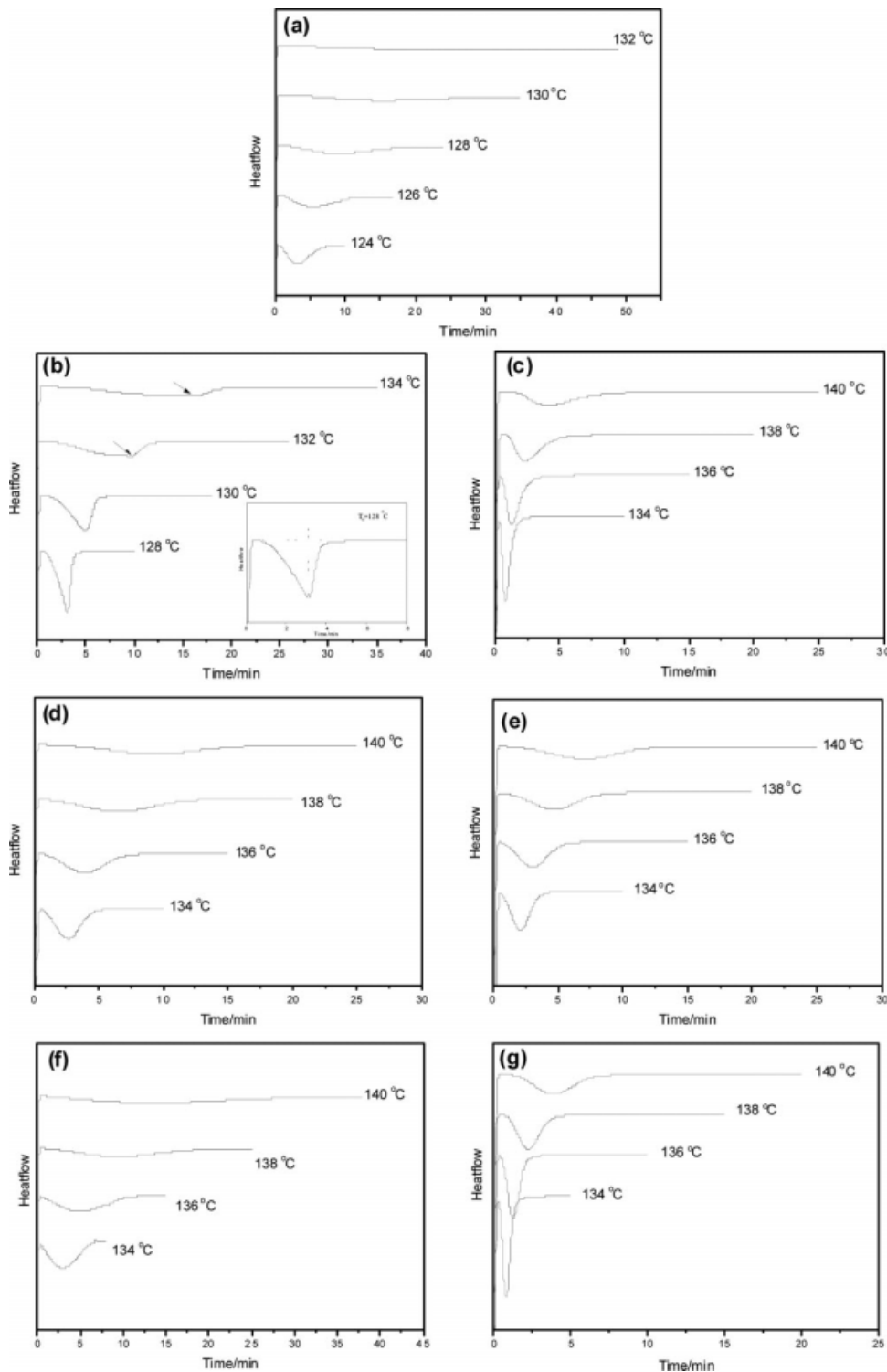


Figure 4 DSC heat flow curves of virgin PP and PP nucleated with different NAs. (a) Virgin PP, (b) PP/0.1DM, (c) PP/0.2DM, (d) PP/0.1TM, (e) PP/0.2TM, (f) PP/0.1DM/0.1TM, and (g) PP/0.2DM/0.2TM.

and PP/0.1DM/0.1TM. Apparently, PP/0.1TM crystallizes faster than PP/0.1DM/0.1TM. The difference of crystallization rate between PP/0.1TM and PP/0.1DM/0.1TM becomes more apparent at elevated crystallization temperatures. In other words, the presence of 0.1 wt % DMDDBS prevents the crystalli-

zation of PP/0.1TM. Once the NA content is up to 0.2 wt %, a reverse crystallization phenomenon has been found. PP/0.2DM/0.2TM has the highest crystallization rate than PP/0.2DM and PP/0.2TM, and PP/0.2TM shows the lowest crystallization rate. It is possible that the presence of 0.2 wt % TMB-5

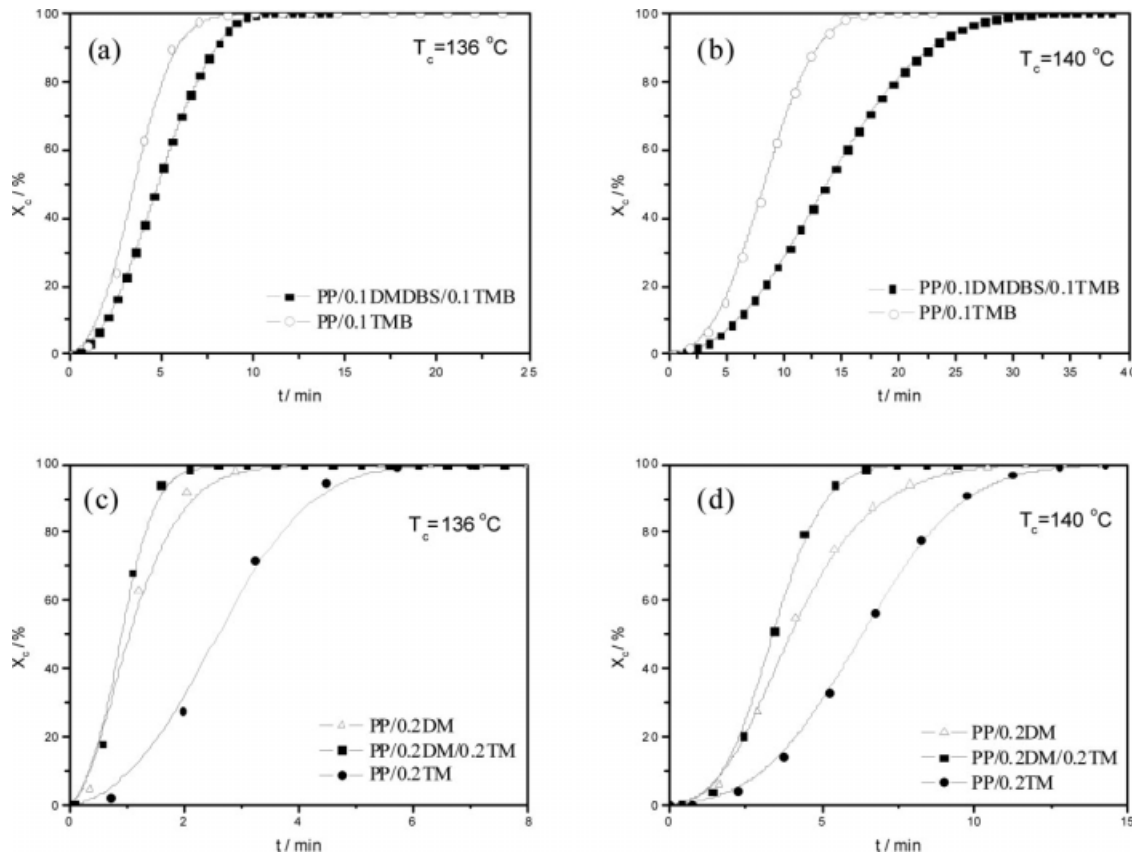


Figure 5 Comparison of the relative crystallization fraction X_c (%) at same isothermal crystallization temperatures T_c between PP with single NA and PP with compounding NAs.

accelerates the crystallization rate of PP/0.2DM. Similarly, enhancing crystallization temperature results in more apparent difference of crystallization rates between PP/0.2DM/0.2TM and PP/0.2DM.

The isothermal crystallization of polymers can usually be well described by the Avrami equation^{35–37}:

$$1 - X_t = \exp(-Kt^n) \quad (3)$$

Here X_t is the relative degree of crystallinity at time t , n is the “Avrami exponent,” which depends on the type of nucleation and the growth mechanism during the crystallization, and K is a rate constant related to nucleation and growth rate parameters. One should notice that the validity of eq. (3) based on the presupposition that the type of crystallization (crystal modification, dimension of growth, nucleation, and growth conditions, respectively) does not change during the whole crystallization. According to the Avrami equation, one formula can be got as follows:

$$\lg[-\ln(1 - X_t)] = n \lg t + \lg K \quad (4)$$

And generally, the plot of $\lg[-\ln(1 - X_t)]$ versus $\lg t$ is a straight line. The slope of the line is n and the intercept with the ordinate yields $\lg K$. From

eq. (3), the crystallization half-time $t_{1/2}$ can be obtained by

$$t_{1/2} = \left(\frac{\ln 2}{k}\right)^{1/n} \quad (5)$$

Figure 6 shows the plots of $\lg[-\ln(1 - X_t)]$ versus $\lg t$ of virgin PP and nucleated PP, and the isothermal crystallization kinetics parameters are shown in Table II. It is evident that for virgin PP the plots exhibit straight lines in the whole crystallization. For PP/0.1DM and PP/0.2DM samples, the plots of them are not simple straight lines and show totally contrary variation trends. For PP/0.1DM, the plots show the initial linear portion, subsequently tends to level up, another linear portion. The increase of slope means that at later crystallization stage the initial crystallization scheme is replaced by another faster one. The similar results have been observed in our previous work, and the reason for the slope increase is ascribed to the crystallizing cluster formation induced by gel network of DMDBS at later crystallization stage.²⁵ For PP/0.2DM, the plots show also the initial linear portion, however, subsequently tends to level off. The decrease of slope means

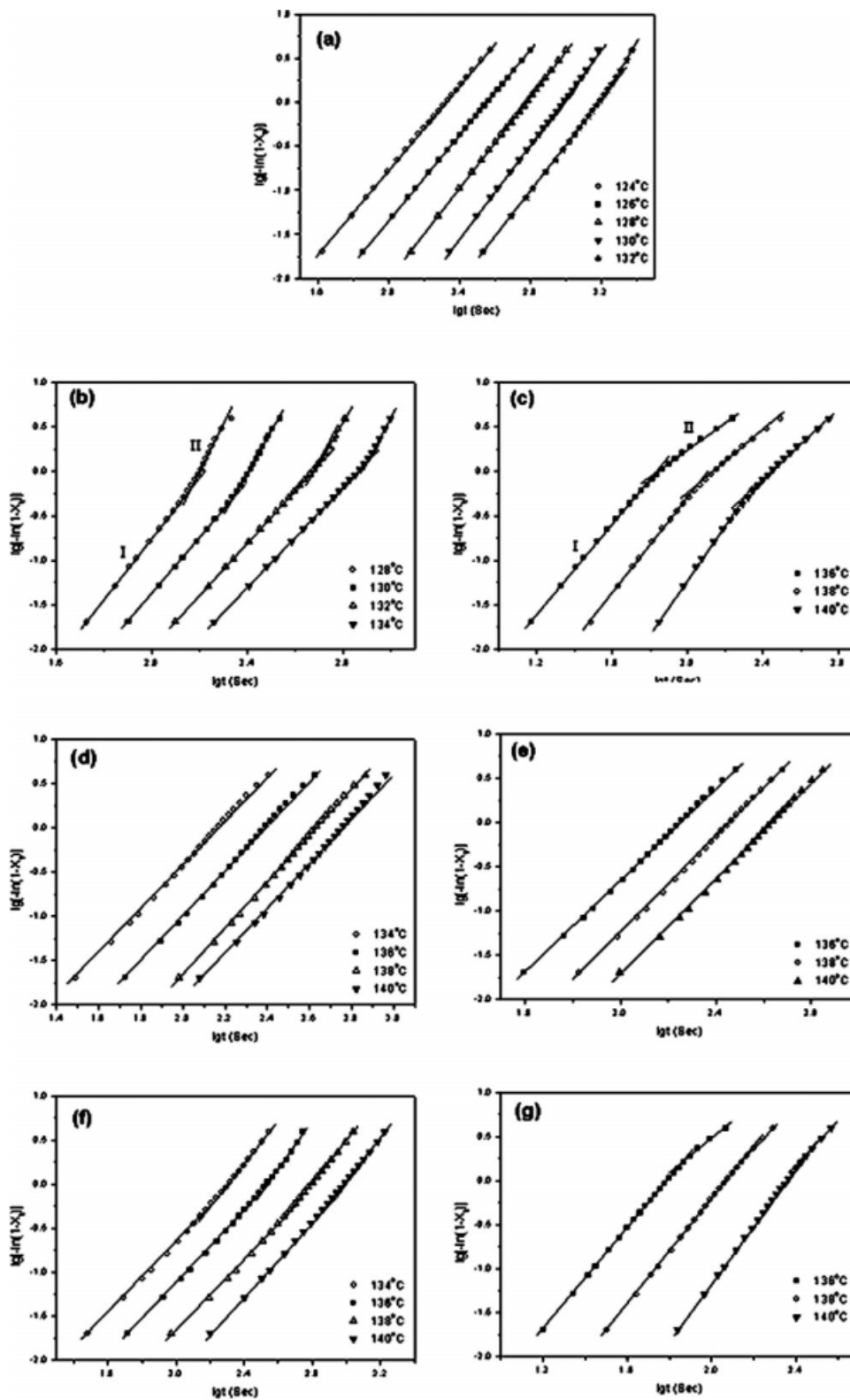


Figure 6 Avrami plots of $\lg[-\ln(1 - X_t)]$ versus $\lg t$ for (a) virgin PP, (b) PP/0.1DM, (c) PP/0.2DM, (d) PP/0.1TM, (e) PP/0.2TM, (f) PP/0.1DM/0.1TM, and (g) PP/0.2DM/0.2TM.

inversely that the initial crystallization scheme is replaced by another slower one. It has been identified that for PP, this slope change (slope decrease) is associated with the impingement of neighboring

spherulites, and thus, represents a beginning of secondary crystallization.³⁸

For PP/0.1TM and PP/0.2TM samples, the plots exhibit straight lines in the whole crystallization,

TABLE II
Isothermal Crystallization Kinetic Parameters of Virgin PP
and PP Nucleated with Different NAs

Sample	T_c (°C)	$t_{1/2}$ (min)	n	\bar{n}^a	$\lg K(T)$	σ_e (mJ/m ²)	K_g ($\times 10^{-5}$) (K ²)
PP	124	3.0	2.44	2.54	-5.6663	166.0	8.27
	126	5.1	2.43		-6.1954		
	128	8.6	2.60		-7.2144		
	130	14.0	2.63		-7.8535		
	132	22.6	2.58		-8.2421		
PP/0.1DM	128	2.5	3.48	3.12	-7.7197	220.5	11.30
	130	4.0	3.21		-7.8134		
	132	6.8	2.96		-7.8958		
	134	10.7	2.81		-8.0458		
PP/0.2DM	134	0.5	2.55	2.66	-4.0255	57.4	2.72
	136	1.0	2.52		-4.6333		
	138	1.9	2.65		-5.6108		
	140	3.9	2.92		-7.0642		
PP/0.1TM	134	2.2	2.49	2.55	-5.4216	62.3	2.66
	136	3.6	2.57		-6.1444		
	138	6.3	2.62		-6.9203		
	140	8.3	2.51		-6.9348		
PP/0.2TM	136	2.6	2.60	2.65	-5.8700	66.3	2.85
	138	4.3	2.69		-6.6365		
	140	6.4	2.67		-7.0592		
PP/0.1DM/0.1TM	134	2.9	2.05	2.09	-4.7605	105.0	4.57
	136	4.9	2.08		-5.2914		
	138	9.2	2.06		-5.8063		
	140	14.1	2.16		-6.4833		
PP/0.2DM/0.2TM	134	0.5	2.65	2.96	-4.0672	54.6	2.58
	136	0.9	2.90		-5.1779		
	138	1.7	3.00		-6.2085		
	140	3.4	3.30		-7.7638		

^a \bar{n} Indicates the average value of n for each sample.

which indicates that Avrami equation can satisfactorily describe the isothermal crystallization of PP with TMB-5 and suggests that the crystallization of PP nucleated with TMB-5 is a one-step process. For PP/0.1DM/0.1TM, the plots are mostly linear portion but with a slight increase of slopes. This suggests that at very later crystallization stage the crystallization of PP/0.1DM/0.1TM becomes faster, indicating a few DMDBS gel network formation and inducing PP crystallization. The plots of PP/0.2DM/0.2TM are also mostly linear portion but with a slight decrease of slopes, which suggests that the crystallization becomes slower at very later crystallization stage.

The crystallization kinetics parameters shown in Table II suggest that NAs accelerate the crystallization process of PP greatly. PP/0.1TM has much smaller $t_{1/2}$ than PP/0.1DM, suggesting the faster crystallization process. However, PP/0.1DM/0.1TM gives slightly higher $t_{1/2}$ value compared with PP/0.1TM. The $t_{1/2}$ value of PP/0.2DM is much smaller than that of PP/0.2TM and is very close to that of PP/0.2DM/0.2TM. This also indicates that the crystallization of PP/0.2DM/0.2TM is similar to that of PP/0.2DM. For all the samples, the Avrami exponent value n ranges from 2 to 3, indicating that

spherulite development arises from an athermal heterogeneous nucleation.³⁹ For virgin PP, it can be ascribed to a heterogeneous nucleation followed by diffusion-controlled spherulite growth because of the existences of impurities and catalyst residues.⁴⁰ It is very interesting that, for PP/0.1DM/0.1TM, the average value of n (\bar{n}) is close to 2, whereas the value of \bar{n} for both PP/0.1DM and PP/0.1TM is close to 2.5. Previous research about the nonisothermal crystallization behavior of PP with compounding DMDBS and TMB-5 NAs has been shown that the nucleation and growth of β -PP is faster than that of α -PP.⁴¹ At low DMDBS concentrations (0.1 wt %), the gel network of DMDBS only forms at later crystallization stage of PP. In this condition, the presence of DMDBS indeed prevents the nucleation role of TMB-5 or the growth of well-developed β -spherulites is prevented or delayed by some embedded tiny α -spherulites, which results in only bundle-like crystalline morphology development. Compared with PP/0.1TM, the β -PP crystal growth mechanism of PP/0.1DM/0.1TM at the initial crystallization stage changes and PP chains only fold freely in the region without DMDBS. Therefore, the decrease of n with the addition of 0.1 wt % DMDBS into PP/0.1TM can be contributed to the folding of PP chains

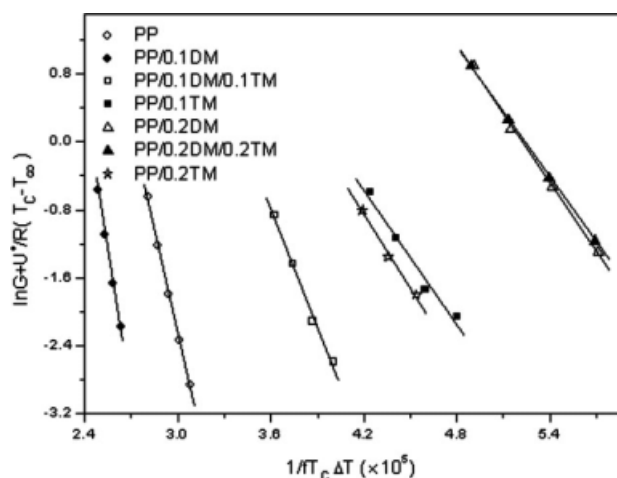


Figure 7 Plots of $\ln G + U^*/R(T_c - T_\infty)$ versus $1/T_c \cdot \Delta T \cdot f$ for virgin PP and PP with different NAs.

and lamellar growth in the restrained region. However, for PP/0.2DM/0.2TM, nanofibrillar 0.2 wt % DMDBS yields a three-dimensional network prior to PP crystallization, and then DMDBS predominates over TMB-5 in controlling both the nucleation and the growth of PP during crystallization. That's why the value of \bar{n} for PP/0.2DM/0.2TM is comparable to that of PP/0.2DM.

The Hoffman–Lauritzen mode has been widely applied to quantify polymer crystallization kinetics in the melt.^{42,43}

$$G = G_0 \exp \left[\frac{-U^*}{R(T_c - T_\infty)} \right] \exp \left[\frac{-K_g}{T_c \cdot \Delta T \cdot f} \right] \quad (6)$$

$$\ln G + \frac{U^*}{R(T_c - T_\infty)} = \ln G_0 - \frac{K_g}{T_c \cdot \Delta T \cdot f} \quad (7)$$

where G_0 is a constant independent of temperature; U^* represents the activation energy characteristic of the transport of the crystallizing segments across the liquid-crystal interface, universally $U^* = 6280$ J/mol; R is the gas constant; T_c is defined as in eq. (2); T_∞ is the theoretical temperature below which all motions associated with the viscous flow ceases and is defined as $T_\infty = T_g - 30\text{K}$; ΔT is the undercooling ($\Delta T = T_m^0 - T_c$), here T_m^0 is defined as in eq. (2); f is a corrective factor responsible for the variation of the equilibrium melting enthalpy with temperature, defined as $f = \frac{2T_c}{T_m^0 + T_c}$; and K_g is nucleation parameter as defined as

$$K_g = 4b_0\sigma\sigma_e T_m^0 / \Delta h_f k \quad (8)$$

where b_0 is the monolayer thickness, σ is the lateral surface free energy, σ_e is the fold surface free energy, k is the Boltzmann constant, and Δh_f is the enthalpy of fusion.

Equations (6)–(8) are applied for crystallization occurring in regimes I and III. From eq. (7), the slop of plot of $\ln G + U^*/R(T_c - T_\infty)$ versus $1/T_c \cdot \Delta T \cdot f$ is K_g . From eq. (8), K_g can be used to obtain the fold surface free energy σ_e . The plots of $\ln G + U^*/R(T_c - T_\infty)$ versus $1/T_c \cdot \Delta T \cdot f$ for virgin PP and PP with different NAs and corresponding K_g values are shown in Figure 7 and Table II, respectively. Prior to determining σ_e , σ is estimated through using the following equation:

$$\sigma = \alpha(a_0 b_0)^{1/2} \Delta h_f \quad (9)$$

where α is derived empirically to be 0.1 and $a_0 b_0$ is the cross-sectional area of the chain.⁴⁴ For α -phase PP, the crystal growth is estimated in favor along (110) lattice plane during melt-crystallization; for β -phase PP, the crystal growth is estimated in favor along (300) lattice plane. The value of Δh_f is 1.96×10^8 J/m³ and 1.77×10^8 J/m³ for α -phase and β -phase, respectively. The cross-sectional area parameters are shown in Table III.^{44–46}

The fold surface free energy σ_e of virgin PP and nucleated PP is shown in Table II too. Except for PP/0.1DM sample, in which the presence of 0.1 wt % DMDBS results in the increase of K_g and σ_e values, the addition of individual NA or compounding NAs results in smaller K_g and σ_e values. Generally, surface nucleation barrier is positive proportion to K_g ⁴³ and the increase of σ_e goes against the folding of the molecule chain.³⁴ Beck's theory thought that a good NA reduced the interfacial surface free energy.¹⁸ The smaller the σ_e value, the better the nucleation effect of NA is. Table II shows that TMB-5 has good nucleation effect for PP; however, the nucleation effect of DMDBS depends on the composition. Only when DMDBS content achieves to a critical value, it has a good nucleation effect for PP crystallization; otherwise, it prevents the crystallization process of PP.¹⁵ PP/0.1DM/0.1TM has bigger σ_e and K_g values than those of PP/0.1TM, which also proves that the presence of 0.1 wt % DMDBS in PP/0.1TM prevents the crystallization process of PP. Similarly, PP/0.2DM/0.2TM has smaller σ_e and K_g values than those of PP/0.2DM and PP/0.2TM,

TABLE III
Growth Plane Parameters of α -Phase PP and β -Phase PP

		(110) Growth plane	σ (mJ/m ²)
α -PP	a_0 (m)	5.49×10^{-10}	11.49
	b_0 (m)	6.26×10^{-10}	
	$a_0 b_0$ (m ²)	3.437×10^{-19}	
(300) Growth plane			
β -PP	a_0 (m)	6.36×10^{-10}	10.48
	b_0 (m)	5.51×10^{-10}	
	$a_0 b_0$ (m ²)	3.504×10^{-19}	

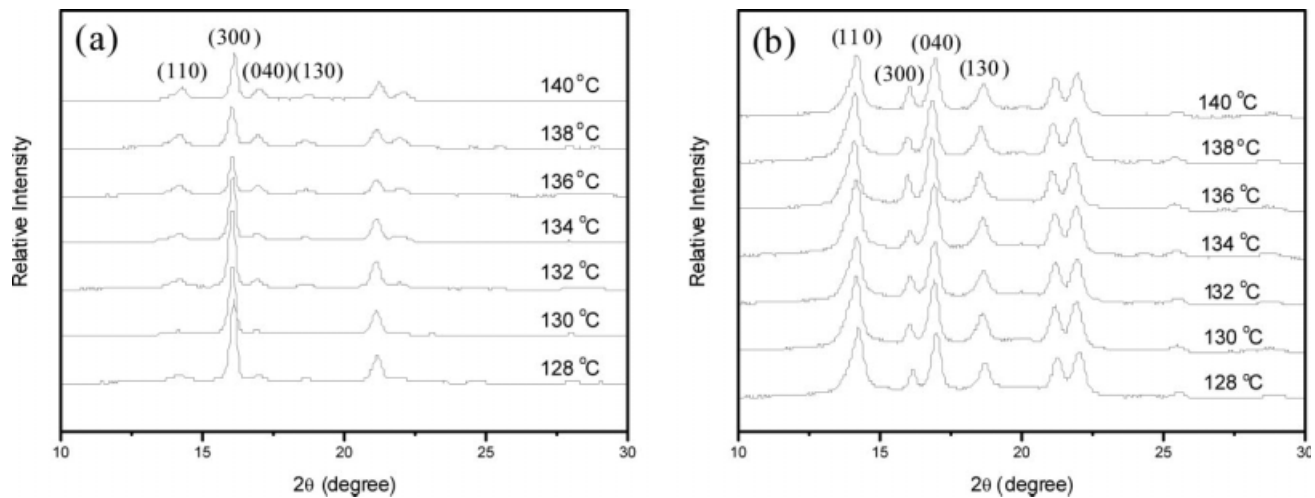


Figure 8 WAXD profiles of (a) PP/0.1DM/0.1TM and (b) PP/0.2DM/0.2TM. Samples were obtained through isothermal crystallization at different temperatures indicated.

indicating the best nucleation effect of such compounding NAs. The lowering of σ_e with the addition of certain NA can be due to the occurrence of multiple nucleations, leading to the formation of loops and tie molecules, and dangling chain ends from primary and secondary crystallization.¹⁶

It should be mentioned that, although K_g and σ_e values increase, the $t_{1/2}$ slightly decreases with the introduction of 0.1 wt % DMDBS into PP compared with virgin PP, (seen in Table II). In other words, both surface nucleation and regular folding of PP chains are hindered; however, the crystallization rate is slightly accelerated. It seems contradictory. However, one should notice that $t_{1/2}$ is calculated from Avrami equation, which is based on a very important hypothesis, i.e., the type of crystallization (crystal modification, dimension of growth, nucleation, and growth conditions, respectively) does not change during the whole crystallization. As discussed earlier, 0.1 wt % DMDBS forms the physical gel network and accelerates the nucleation rate of PP with the prolongation of crystallization time, which will change the crystallization mechanism of PP and leads to smaller $t_{1/2}$ for PP/0.1DM sample. Smith and coworkers have proved that DMDBS is inactive as a NA when presents at very low concentrations (<0.1 wt %), not because of destruction of the additive, but simply because it acts merely as a high-melting (poor) solvent in the relevant temperature regime.¹⁵

Crystallization structure

The aforementioned results show that the melting and isothermal crystallization behaviors of PP/0.1DM/0.1TM are close to those of PP/0.1TM, and PP/0.2DM/0.2TM close to PP/0.2DM. In other

words, 0.1 wt % TMB-5 shows better nucleation effect than 0.1 wt % DMDBS in PP/0.1DM/0.1TM sample, and PP crystallizes mainly nucleated by 0.1 wt % TMB-5; however, PP crystallizes mostly affected by 0.2 wt % DMDBS rather than by 0.2 wt % TMB-5 in PP/0.2DM/0.2TM sample. To further prove this, WAXD are applied to investigate the crystal structure of PP with compounding NAs. Figure 8 shows the WAXD profiles of PP/0.1DM/0.1TM and PP/0.2DM/0.2TM. The relative β -phase content is calculated and the data are shown in Figure 9. It can be observed from Figures 8 and 9 that β -phase formation is the main crystallization characteristic in PP/0.1DM/0.1TM sample, and α -phase PP is the determinable crystalline structure in PP/0.2DM/0.2TM sample. Figure 9 also shows the different variation trends of relative β -phase content in PP/0.1DM/0.1TM and PP/0.2DM/0.2TM samples.

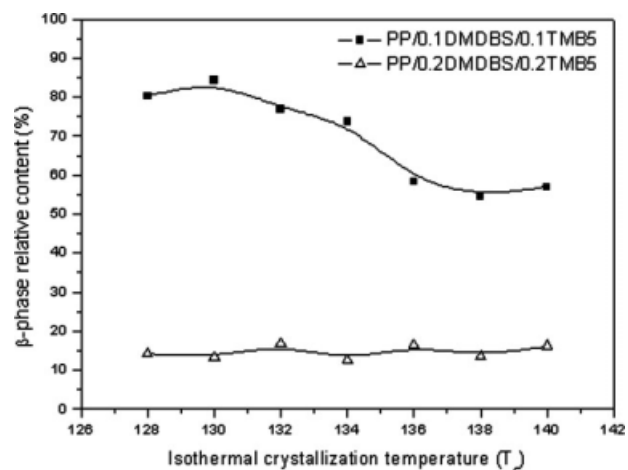


Figure 9 Relative content of β -phase in PP with compounding NAs obtained at different isothermal crystallization temperatures.

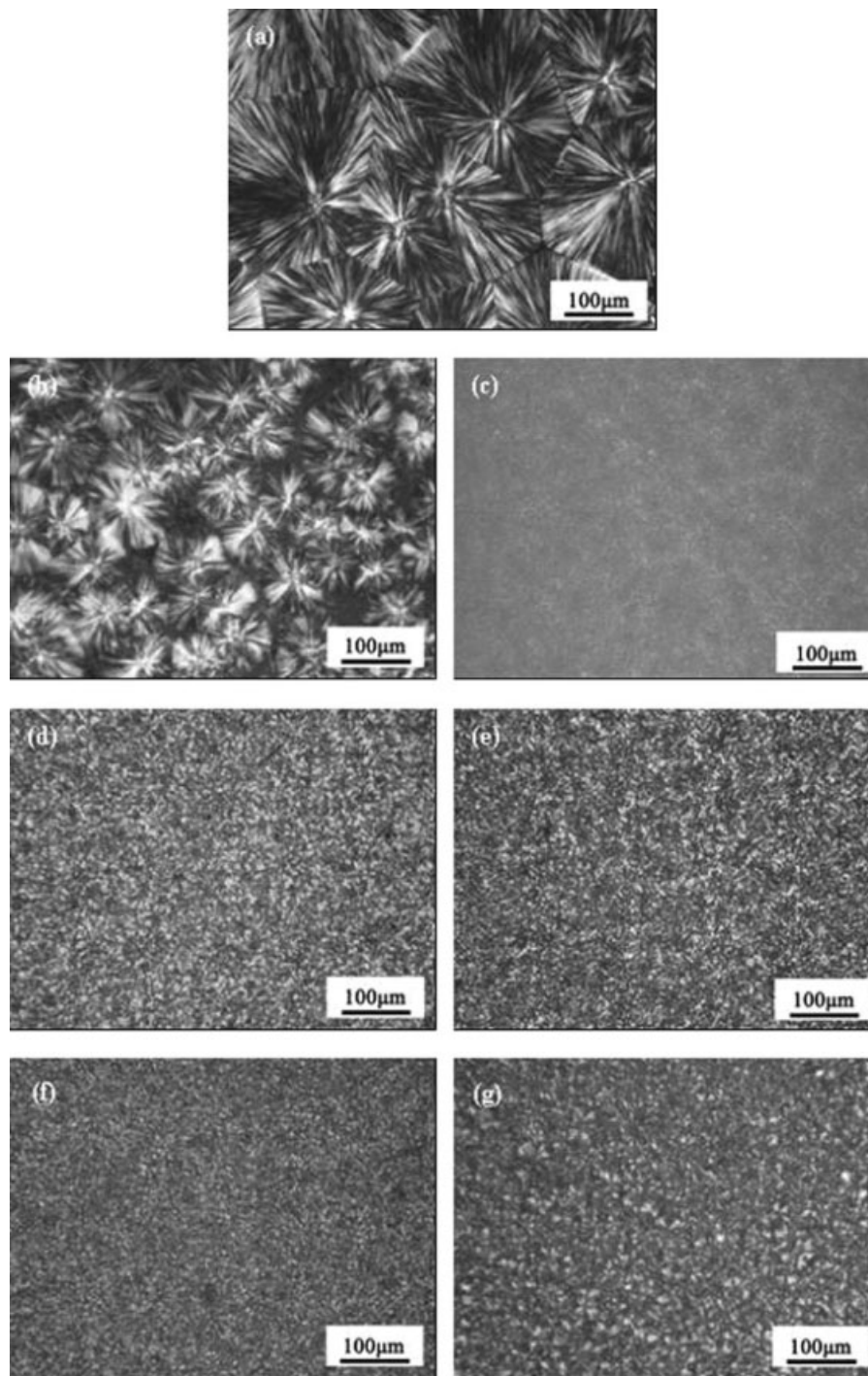


Figure 10 PLM photographs of isothermal crystallization morphologies of virgin PP and PP with different NAs. (a) Virgin PP, (b) PP/0.1DM, (c) PP/0.2DM, (d) PP/0.1TM, (e) PP/0.2TM, (f) PP/0.1DM/0.1TM, and (g) PP/0.2DM/0.2TM.

Increasing isothermal crystallization temperature reduces the relative β -phase content in the former sample, which indicates that the high crystallization temperature is unfavorable for the nucleation and growth of β -phase.⁴⁷ However, the latter sample shows that the relative β -phase content is independent of the crystallization temperature (128–140°C), which can be attributed to one thing that high TMB-

5 content always shows certain nucleation effect for PP crystallization, although the nucleation effect of DMDBS is more apparent and decisive to the crystallization of most PP.

The crystallization morphologies of virgin PP and nucleated PP are observed by polarized light microscopy (PLM) and the results are shown in Figure 10. Obviously, the addition of NA reduces the spherulites

TABLE IV
Lamellar Thickness (L_m) of Virgin PP and PP
Nucleated with NAs Formed During the
Isothermal Crystallization Process

Sample	T_c (°C)	T_m^M (°C)	T_m^o (°C)	L_m (nm)
PP	124	162.6	195.5	24.14
	126	163.4		24.77
	128	164.4		25.57
	130	165.3		26.28
	132	166.3		27.19
PP/0.1DM	128	164.1	209.5	23.93
	130	165.1		24.46
	132	166.3		25.12
	134	167.4		25.82
	136	164.6		34.46
PP/0.2DM	138	164.9	172.2	36.07
	140	165.4		38.76
	134	155.2		178.7
PP/0.1TM	136	156.2	178.7	14.18
	138	157.1		14.75
	140	158.4		15.73
	134	155.2		181.1
PP/0.2TM	136	156.4	181.1	13.80
	138	157.3		14.30
	140	158.6		15.15
	134	154.1		186.9
PP/0.1DM/0.1TM	136	155.4	186.9	17.32
	138	156.7		18.08
	140	157.8		18.71
	136	164.7		172.3
PP/0.2DM/0.2TM	138	165.1	172.3	34.47
	140	165.6		36.97

greatly as expected. Furthermore, the crystallization morphologies of PP/0.1DM/0.1TM and PP/0.2DM/0.2TM are similar to those of PP/0.1TM and PP/0.2DM, respectively, as obtained from DSC and WAXD measurement.

As well known to all that the crystallization temperature influences the nucleation and growth of lamellar, and inversely the lamellar thickness influences the melting behavior of the polymer crystals, i.e., melting peak temperature. Thomson and Gibbs developed an equation to describe this relationship⁴⁸:

$$T_m = T_m^o \left(1 - \frac{2\sigma_e}{l\Delta h_f} \right) \quad (10)$$

where l is the lamellar thickness, T_m , σ_e , and Δh_f are defined as previous. According to Thomson–Gibbs equation, the lamellar thickness of a polymer can be calculated as follows:

$$l = \frac{2\sigma_e T_m^o}{\Delta h_f (T_m^o - T_m)} \quad (11)$$

The lamellar thickness of virgin PP and nucleated PP obtained during the isothermal crystallization process are calculated and the results are shown in Table IV. Here the T_m^o and σ_e values corresponding

to the main melting peak of PP and nucleated PP obtained above is applied to calculate the lamellar thickness. Obviously, α -phase shows bigger lamellar thickness than that of β -phase, and lamellar thickness increases with the increasing of crystallization temperature.⁴⁹ Increasing the TMB-5 content in PP matrix results in the decrease of lamellar thickness. For PP nucleated with DMDBS, the effect of DMDBS content on lamellar thickness cannot be directly deduced because of the crystallization taking place at different temperatures. But in literatures gradually decreasing of lamellar thickness with increasing DMDBS content has been reported.¹⁹ Furthermore, Table IV shows that the presence of 0.1 wt % DMDBS in PP/0.1DM/0.1TM increases the lamellar thickness of β -phase, which may be ascribed to the presence of DMDBS reduces the growth rate of β -phase and leaves enough time for lamellar growth; however, the presence of 0.2 wt % TMB-5 reduces the lamellar thickness of α -phase in PP/0.2DM/0.2TM. Factually, 0.2 wt % TMB-5 has a good nucleation effect for PP crystallization. During the crystallization process, the presence of small β -phase crystalline prevents the growth of α -phase lamellar nucleated by 0.2 wt % DMDBS, which results in the thinner lamellar formation. Further work is proceeding now to understand how DMDBS or TMB-5 affects the growth of lamellar in nucleated PP with compounding NAs.

CONCLUSIONS

In summary, the melting and isothermal crystallization behaviors of virgin PP and nucleated PP were comparatively investigated in detail. The results show that the addition of individual NA influences the crystallization rate of PP apparently. For PP/DMDBS system, the crystallization behavior depends on the DMDBS content severely. However, for PP/TMB-5 system, either 0.1 or 0.2 wt % TMB-5 shows good nucleation effect for PP crystallization. The crystallization and melting behaviors of PP with compounding NAs are greatly dependent on the composition of compounding NAs. In PP/0.1DM/0.1TM sample, TMB-5 shows more apparent nucleation effect and PP crystallizes mainly nucleated by TMB-5, and in this condition, β -phase formation is the main crystallization characteristic. In PP/0.2DM/0.2TM sample, DMDBS takes up determinable nucleation role for PP, and α -phase is the main crystallization structure. Our results shed light on one thing that one can obtain any ration of α -phase content to β -phase content through selecting the available NA and controlling the composition of compounding NAs.

References

1. Zhang, P. Y.; Liu, X. X.; Li, Y. Q. *Mater Sci Eng A* 2006, 434, 310.
2. Varga, J. *J Macromol Sci Part B: Phys* 2002, 41, 1121.
3. Kotek, J.; Raab, M.; Eichhorn, J.; Grellmann, W. *J Appl Polym Sci* 2002, 85, 1174.
4. Raab, M.; Študla, J.; Kolařík, J. *Eur Polym Mater* 2004, 40, 1317.
5. Kotek, J.; Kelnar, I.; Baldrian, J.; Raab, M. *Eur Polym Mater* 2004, 40, 679.
6. Meille, S. V.; Ferro, D. R.; Bruckner, S.; Lovinger, A. J.; Pad-den, F. J. *Macromolecules* 1994, 27, 2615.
7. Huo, H.; Jiang, S. C.; An, L. J.; Feng, J. C. *Macromolecules* 2004, 37, 2478.
8. Varga, J.; Karger-Kocsis, J. *J Polym Sci Part B: Polym Phys* 1996, 34, 657.
9. Wu, C. M.; Chen, M.; Karger-Kocsis, J. *Polymer* 1999, 40, 4195.
10. Li, H. H.; Jiang, S. D.; Wang, J. J.; Wang, D. J.; Yan, S. K. *Macromolecules* 2003, 36, 2802.
11. Fujiwara, Y. *Colloid Polym Sci* 1975, 253, 273.
12. Zhang, Y. F.; Xin, Z. *J Polym Sci Part B: Polym Phys* 2007, 45, 590.
13. Romankiewicz, A.; Tomasz, S.; Brostow, W. *Polym Int* 2004, 53, 2086.
14. Tenma, M.; Yamaguchi, M. *Polym Eng Sci* 2007, 47, 1141.
15. Kristiansen, M.; Werner, M.; Tervoort, T.; Smith, P.; Blumenhofer, M.; Schmidt, H.-W. *Macromolecules* 2003, 36, 5150.
16. Feng, Y.; Jin, X.; Hay, J. N. *J Appl Polym Sci* 1998, 69, 2089.
17. Zhou, Z.; Wang, S. F.; Lu, L.; Zhang, Y.; Zhang, Y. X. *J Polym Sci Part B: Polym Phys* 2007, 45, 1616.
18. Beck, H. N. *J Appl Polym Sci* 1975, 19, 371.
19. Romankiewicz, A.; Sterzynski, T. *Macromol Symp* 2002, 180, 241.
20. Shepard, T. A.; Delsorbo, C. R.; Louth, R. M.; Walborn, J. L.; Norman, D. A.; Harvey, N. G.; Spontak, R. J. *J Polym Sci Part B: Polym Phys* 1997, 35, 2617.
21. Yamasaki, S.; Ohashi, Y.; Tsutsumi, H.; Tsujii, K. *Bull Chem Soc Jpn* 1995, 68, 146.
22. Nogales, A.; Mitchell, G. R.; Vaughan, A. S. *Macromolecules* 2003, 36, 4898.
23. Kristiansen, M.; Tervoort, T.; Smith, P. *Polymer* 2003, 44, 5885.
24. Nogales, A.; Olley, R. H.; Mitchell, G. R. *Macromol Rapid Commun* 2003, 24, 496.
25. Wang, Y.; Gao, Y.; Shi, J. *J Appl Polym Sci* 2008, 107, 309.
26. Turner-Jones, A.; Aizlewood, J. M.; Beckett, D. R. *Makromol Chem* 1964, 75, 134.
27. Li, J. X.; Cheung, W. L. *Polymer* 1998, 39, 6935.
28. Passingham, C.; Hendra, P. J.; Cudby, M. E. A.; Zichy, V.; Weller, M. *Eur Polym Mater* 1990, 26, 631.
29. Wang, K. F.; Mai, K. C.; Zeng, H. M. *J Appl Polym Sci* 2000, 78, 2547.
30. Marco, C.; Ellis, G.; Gómez, M. A.; Arribas, J. M. *J Appl Polym Sci* 2003, 88, 2261.
31. Fillon, B.; Thierry, A.; Wittmann, J. C.; Lotz, B. *J Polym Sci Part B: Polym Phys* 1993, 31, 1407.
32. Zhang, R. H.; Shi, D.; Tjong, S. C.; Li, R. K. Y. *J Polym Sci Part B: Polym Phys* 2007, 45, 2674.
33. Hoffman, J. D.; Weeks, J. J. *J Chem Phys* 1962, 37, 1723.
34. Hoffman, J. D. *Polymer* 1983, 24, 3.
35. Avrami, M. *J Chem Phys* 1939, 7, 1103.
36. Avrami, M. *J Chem Phys* 1940, 8, 212.
37. Avrami, M. *J Chem Phys* 1941, 9, 177.
38. Wunderlich, B., Ed. *Macromolecular Physics*; Academic Press: New York, 1976; Vol. 2, Chapter 6, pp 118–270.
39. Avalos, F.; Lopez-Manchado, M. A.; Arroyo, M. *Polymer* 1998, 39, 6173.
40. López-Manchado, M. A.; Biagiotti, J.; Torre, L.; Kenny, J. M. *Polym Eng Sci* 2000, 40, 2194.
41. Bai, H. W.; Wang, Y.; Liu, L.; Zhang, J. H.; Han, L. *J Polym Sci Part B: Polym Phys* 2008, 46, 1853.
42. Lauritzen, J. I.; Hoffman, J. D. *J Appl Phys* 1973, 44, 4340.
43. Hoffman, J. D.; Davis, G. T.; Lauritzen, J. I. In *Treatise on Solid State Chemistry*; Hannay, N. B., Ed.; Plenum Press: New York, 1976; Vol. 3, Chapter 7, pp 497–614.
44. Clark, E. J.; Hoffman, J. D. *Macromolecules* 1984, 17, 878.
45. Varga, J. In *Polypropylene Structure, Blends and Composites*; Karger-Kocsis, J. Ed.; Chapman and Hall: London, 1995; Vol. 1, Chapter 3, pp 56–115.
46. Karger-Kocsis, J.; Varga, J.; Ehrenstein, G. W. *J Appl Polym Sci* 1997, 64, 2057.
47. Varga, J.; Mudra, I.; Ehrenstein, G. W. *J Appl Polym Sci* 1999, 74, 2357.
48. Bershtein, V. A.; Egorov, V. M. *Differential Scanning Calorimetry of Polymers: Physics, Chemistry, Analysis*. Ellis Horwood: London, 1994.
49. Zhu, X. Y.; Yan, D. Y.; Tan, S. S.; Wang, T.; Yan, D. H.; Zhou, E. L. *J Appl Polym Sci* 2000, 77, 163.